

Validating Serum S100B and Neuron-Specific Enolase as Biomarkers for the Human Brain – A Combined Serum, Gene Expression and MRI Study

Daniel-Paolo Streitbürger^{1*}, Katrin Arelin^{1,2,3}, Jürgen Kratzsch⁴, Joachim Thiery^{3,4}, Johann Steiner^{5,6}, Arno Villringer^{1,2,3}, Karsten Mueller¹✉, Matthias L. Schroeter^{1,2,3,7}✉

1 Max Planck Institute for Human Cognitive and Brain Sciences, Leipzig, Germany, **2** Clinic for Cognitive Neurology, University of Leipzig, Leipzig, Germany, **3** Leipzig Research Center for Civilization Diseases, University of Leipzig, Leipzig, Germany, **4** Institute of Laboratory Medicine, Clinical Chemistry and Molecular Diagnostics, University of Leipzig, Leipzig, Germany, **5** Department of Psychiatry, University of Magdeburg, Magdeburg, Germany, **6** Pembroke College, University of Cambridge, Cambridge, United Kingdom, **7** Consortium for Frontotemporal Lobar Degeneration, Ulm, Germany

Abstract

Introduction: Former studies have investigated the potential of serum biomarkers for diseases affecting the human brain. In particular the glial protein S100B, a neuro- and gliotrophin inducing plasticity, seems to be involved in the pathogenesis and treatment of psychiatric diseases such as major depression and schizophrenia. Neuron-specific enolase (NSE) is a specific serum marker for neuronal damage. However, the specificity of these biomarkers for cell type and brain region has not been investigated in vivo until now.

Methods: We acquired two magnetic resonance imaging parameters sensitive to changes in gray and white matter (T₁-weighted/diffusion tensor imaging) and obtained serum S100B and NSE levels of 41 healthy subjects. Additionally, we analyzed whole brain gene expressions of S100B in another male cohort of three subjects using the Allen Brain Atlas. Furthermore, a female post mortal brain was investigated using double immunofluorescence labelling with oligodendrocyte markers.

Results: We show that S100B is specifically related to white matter structures, namely the corpus callosum, anterior forceps and superior longitudinal fasciculus in female subjects. This effect was observed in fractional anisotropy and radial diffusivity – the latest an indicator of myelin changes. Histological data confirmed a co-localization of S100B with oligodendrocyte markers in the human corpus callosum. S100B was most abundantly expressed in the corpus callosum according to the whole genome Allen Human Brain Atlas. In addition, NSE was related to gray matter structures, namely the amygdala. This effect was detected across sexes.

Conclusion: Our data demonstrates a very high S100B expression in white matter tracts, in particular in human corpus callosum. Our study is the first in vivo study validating the specificity of the glial marker S100B for the human brain, and supporting the assumption that radial diffusivity represents a myelin marker. Our results open a new perspective for future studies investigating major neuropsychiatric disorders.

Citation: Streitbürger D-P, Arelin K, Kratzsch J, Thiery J, Steiner J, et al. (2012) Validating Serum S100B and Neuron-Specific Enolase as Biomarkers for the Human Brain – A Combined Serum, Gene Expression and MRI Study. PLoS ONE 7(8): e43284. doi:10.1371/journal.pone.0043284

Editor: Bogdan Draganski, Centre Hospitalier Universitaire Vaudois Lausanne - CHUV, UNIL, Switzerland

Received: March 1, 2012; **Accepted:** July 23, 2012; **Published:** August 14, 2012

Copyright: © 2012 Streitbürger et al. This is an open-access article distributed under the terms of the Creative Commons Attribution License, which permits unrestricted use, distribution, and reproduction in any medium, provided the original author and source are credited.

Funding: KA, JT, AV and MLS are supported by LIFE – Leipzig Research Center for Civilization Diseases at the University of Leipzig – funded by the European Union, European Regional Development Fund and by Free State of Saxony within the framework of the excellence initiative. MLS is supported by the German Consortium for Frontotemporal Lobar Degeneration, funded by the German Federal Ministry of Education and Research. The funders had no role in study design, data collection and analysis, decision to publish, or preparation of the manuscript and no additional external funding has been received for this study.

Competing Interests: The authors have declared that no competing interests exist.

* E-mail: paolo@cbs.mpg.de

✉ These authors contributed equally to this work.

Introduction

Former studies investigated the potential of serum proteins as biomarkers for brain diseases. In particular, the glial protein S100B has been discussed in this context [1–3]. S100 proteins influence various cellular responses along the calcium-signal-transduction pathway [2,4,5]. S100B is localized in and may be secreted by astro- and oligodendrocytes. In nanomolar concentrations it acts as growth and/or differentiation factor for neurons

and glia, whereas in micromolar levels S100B may have deleterious effects and induces apoptosis due to an increased expression of proinflammatory cytokines [6,7]. Recently, it has been suggested that S100B may play a crucial role in the pathogenesis and treatment of frequent psychiatric disorders such as major depression and schizophrenia [1,7–13]. Antidepressive drugs lead via the serotonergic system to astrocytic S100B secretion, which in turn may induce neurogenesis required for the behavioral effects of antidepressants [8,14]. Consequently,

S100B-related mechanisms have been proposed as potential targets for novel antidepressive therapies.

Accordingly, one might assume that increased serum S100B might reflect an ongoing regenerative action in neuropsychiatric diseases. However, serum S100B, which might not reflect local concentrations in the brain, was rather elevated in acute stages of depression and schizophrenia and positively correlated with depressive symptoms and negative symptoms in schizophrenia. Accordingly, clinical data suggest serum S100B rather as a pathological biomarker than plasticity marker [7–9]. In agreement with these arguments genetic studies demonstrated that S100B is a susceptibility gene for mood disorders and schizophrenia [1], developmental dyslexia [3] and cognitive dysfunction [15]. In sum, serum S100B may constitute a diagnostic, prognostic and treatment biomarker for major depression, schizophrenia and neurological diseases [16,17]. Beside S100B, neuron-specific enolase (NSE) has been suggested to be a specific serum marker for neuronal damage. Because NSE is primarily localized in the cytoplasm of neurons [18–22] and is not secreted, increases in cerebrospinal fluid or blood indicate structural damage to neuronal cells.

Although serum S100B and NSE offer the opportunity to easily investigate the function of or damage to glial and neuronal structures in neuropsychiatric disorders [8,23,24], the specificity of these biomarkers for cell type and brain region have not been investigated in vivo until now. Magnetic resonance imaging (MRI) is very sensitive in identifying regional structural changes in the human brain. Voxel based morphometry (VBM) [25] has enabled a wide variety of studies focusing on gray matter (GM) changes [26–28] in various diseases [29–32], due to training [33–35] or genetic effects [36–38] using T_1 -weighted images. With another MRI-based approach, diffusion tensor imaging (DTI) [39], one may specifically analyze white matter (WM) changes, for instance with the software package tract-based spatial statistics (TBSS) developed by the Oxford Centre for Functional MRI of the Brain (FMRIB) [40]. In addition to the most important DTI parameter fractional anisotropy (FA) [41] indicating global WM integrity [42], axial and radial diffusivity are markers for axonal and myelin degeneration [43].

Our study aimed to isolate the regional neural correlates of glial (S100B) and neuronal (NSE) serum markers with two MRI parameters sensitive to changes in the GM and WM of the human brain. We hypothesized that S100B as an astro- and oligodendrocytic marker is associated with GM and WM parameters. For the WM, we expected the strongest effect in the corpus callosum, because this structure has an abundance of oligodendrocytes according to histological studies [6] and shows the highest signal-to-noise ratio due to parallel orientation of numerous fibers [44]. Additionally, we hypothesized that NSE as a neuronal marker is associated with GM parameters.

To avoid any influences of diseases on the association between regional MRI markers and serum S100B and NSE, we involved only healthy subjects. It is well known that S100B is age [45–47], sex [46,48] and weight dependent [49–51], while influences of age or sex on NSE are controversially discussed [52–54]. Moreover, recent studies combining serum markers and WM parameters found different results for female and male subjects [44]. To control for these influences, we analyzed data separately in female and male subjects, included a wide age range, and controlled for influences of age, body mass index (BMI) and total intracranial volume (TIV). Finally, we validated our results by additionally investigating gene expression in the whole human brain genome wide atlas of the Allen Institute for Brain Sciences and by

histological co-localization studies in human post mortem brain and in cell culture.

Methods

Subjects

Forty-one healthy Caucasian adults participated in the study (20 male/21 female; mean age $50.35 \pm 21.61/46.38 \pm 24.44$ years; range 21–74/20–79). All participants gave written informed consent. They completed a health history questionnaire. The research protocol was approved by the Ethics Committee of the University of Leipzig, and was in accordance with the latest version of the Declaration of Helsinki.

T_1 -weighted Magnetic Resonance Imaging

Scanning was performed on a 3T TIM Trio device (Siemens Medical Solutions, Erlangen, Germany). T_1 -weighted images were acquired with a three-dimensional magnetization prepared rapid gradient echo (MP-RAGE) sequence using the following parameters: inversion time 650 ms, repetition time (TR) = 1.3 s, TR of the gradient-echo kernel 10 ms, echo time 3.46 ms, flip angle 10° , bandwidth 130 Hz/pixel, acquisition matrix 256×240 , field of view $256 \times 240 \text{ mm}^2$, slab thickness 192 mm (sagittal orientation), 128 partitions, 95% slice resolution. Reconstructed images were obtained with a nominal voxel size of $1 \times 1 \times 1 \text{ mm}^3$.

Diffusion Tensor Imaging

Diffusion-weighted images were acquired with twice-refocused spin echo echo-planar-imaging sequence [46], $TE = 100 \text{ ms}$, $TR = 12 \text{ s}$, 128×128 image matrix, $FOV = 220 \times 220 \text{ mm}^2$: 88 axial slices (no gap); voxel size: $1.72 \times 1.72 \times 1.7 \text{ mm}^3$. Additionally, fat saturation was employed together with 6/8 partial Fourier imaging and generalized auto-calibrating partially parallel acquisitions (GRAPPA [55], acceleration factor = 2). Diffusion weighting was isotropically distributed along 60 diffusion-encoding gradient directions with a b-value of 1000 s/mm^2 .

Measurement of Serum Markers

Blood samples were obtained by venipuncture from subjects. Analysis was performed as previously described in detail [8,9]. S100B and NSE were measured by monoclonal 2-site immunoluminometric assays performed on the fully mechanized system LIAISON (Diasorin, Dietzenbach, Germany). The detection limit for the assays was $0.02 \mu\text{g/l}$ and $0.04 \mu\text{g/l}$.

Voxel Based Morphometry

T_1 -weighted images were processed using VBM8, implemented by Gaser *et al.* (<http://dbm.neuro.uni-jena.de/vbm/>) for the Statistical Parametrical Mapping software (SPM, ver. 8.xx). GM segments were non-linearly registered, modulated [56] and smoothed using a 5 mm^3 smoothing-kernel. Resulting images were fed into a multiple regression model using S100B (or NSE) as regressor of interest and NSE (or S100B), BMI, TIV and age as confounding covariates. GM images were threshold to exclude voxels with a GM probability below 10% prior to the statistical analyses. Significant resulting brain structures were identified by the TD-ICBM Human Atlas [57] and a volume of interest (VOI) analysis over both groups of subjects was created based on this masks. Averaged voxel values were correlated with the obtained biomarker levels using partial correlation in MATLAB (version 7.11.0/R2010b, Natick, Massachusetts: The MathWorks Inc., 2012) controlling for the same parameters as described above. To proof the significance of the difference of the correlation coefficients we used a formula which has been described in [58].

Tract-Based Spatial Statistics

Secondly, we analyzed DTI datasets using TBSS from the FMRIB Software Library (FSL) [40]. We followed the recommended preprocessing steps with default parameters described on their homepage (<http://www.fmrib.ox.ac.uk/fsl/tbss/index.html>). After preprocessing, we fed the images into a multiple regression analysis using FSLs 'randomise' program, with the same statistical design as it is described above and computed a randomize statistics with 100,000 permutations. Results were thresholded by the threshold-free cluster enhancement (TFCE) approach ($p < 0.05$ corrected). TFCE is a technique which aims to enhance cluster-like structures and simultaneously ignores noisy regions in statistical images without explicitly defining a hard-threshold-based clustering [59]. Furthermore, we followed the same VOI statistical procedure for significant identified brain structures as above. Due to the different analyzed tissue we used the anatomical atlas from TD-ICBM Human Atlas to the Johns Hopkins University ICBM white-matter-labels [60]. All statistics, TBSS as well as VOI analysis, were applied on the skeletonized FA, radial (λ_{\perp}) and axial diffusivity data (λ_{\parallel}).

Histological Analyses – Post Mortem and Cell Culture

The brain of a 32 year old Caucasian woman (who died from acute myocarditis associated with lupus without brain involvement), which is not included in our imaging study, was removed from the cranium within 20 hrs after death. A tissue sample from the corpus callosum was fixed in 4% buffered paraformaldehyde (pH 7.4), cryoprotected, and rapidly frozen at -20°C using 2-methylbutane. Serial sagittal 20 μm thick sections were cut on a cryostat (Jung Frigocut 2800 E, Leica, Bensheim, Germany). Oligodendroglial OLN-93 cells were obtained from the Richter-Landsberg lab (Oldenburg, Germany) and cultured as previously described [11]. Free-floating sections or OLN-93 cultures were washed and incubated with the corresponding antibodies: (i) polyclonal rabbit anti-recombinant-S100B 1:50; (ii) monoclonal mouse anti-myelin basic protein 1:100, (iii) monoclonal mouse anti-p75 neurotrophin receptor 1:100 with 0.3% Triton X-100 and 1% normal goat serum overnight at 4°C . This step was followed by incubation for 3 h with the respective secondary antibodies at a 1:500 dilution: Alexa Fluor 546 (goat anti-rabbit-IgG; red fluorescence) and Alexa 488 (goat antimouse-IgG; green fluorescence). Specimens were examined using a fluorescence microscope (Axiophot; Zeiss, Jena, Germany) equipped with phasecontrast, fluorescein and rhodamine optics. The specificity of the immunoreactions was controlled by the application of buffer instead of the primary antiserum.

Whole Brain Genome Expression Analysis

The Allen Human Brain Atlas is a publicly available online resource of gene expression (www.human.brain-map.org; [61]). It characterizes gene expression in human brain tissue with genome-wide microarray-based gene expression profiles including over 62,000 gene probes for 500 samples from each hemisphere covering the whole brain. Tissue samples collected for microarray analysis were processed for RNA isolation, quantification, and normalization. Microarray analysis data, normalized across each brain, are included in the Allen Human Brain Atlas dataset and illustrated in heat map format as z scores. Z scores represent individual regional gene expression normalized to whole brain expression of that gene. When there are multiple samples for a given structure and subject, values in the heat map are average values. Quality control was performed several times. To date, three subjects without a history of neuropsychiatric or neurological conditions are contained in the database (H0351.1009,

H0351.2001, H0351.2002; age 57, 24, 39 years; all male; ethnicity white/Caucasian [1,1009], and black/African American [2,2001/.2002]). Note that these subjects were not included in our imaging study. Detailed information for subjects included and analysis methods is available at www.human.brain-map.org. To calculate mean values of normalized expression in brain regions of interest we extracted normalized z scores from the database for each individual and region of interest. Thereafter, expression values were compared with two-tailed Student's t tests.

Results

Serum Markers

Because serum S100B might be influenced by sex, age and body mass index, we controlled for these factors. In accordance with literature data [48] mean serum S100B levels were higher in female (65.7 ± 26.6 ng/l) compared to male subjects (54.0 ± 16.4 ng/l; 'trend' $p = 0.1$), whereas there were no sex related differences for serum NSE (females 9.68 ± 1.75 $\mu\text{g/l}$; males 10.27 ± 1.96 $\mu\text{g/l}$; $p = 0.31$; two-sample Student's t-test; generally, p values for two tailed tests). Serum S100B and NSE values did not correlate within the group of female subjects ($p = 0.22$), but correlated positively within the group of male subjects ($p < 0.05$; Pearson's correlation). Age and body mass index were not correlated with S100B or NSE if calculated in female and male subjects alone or in the whole group. Accordingly, we analyzed correlations between serum markers as regressors of interest and imaging parameters in both sex groups separately and, in general, controlled for the respective second serum marker beside age and body mass index (and total intracranial volume) as confounding covariates in the following analyses.

Combining Serum Markers and Diffusion Tensor Imaging

Both S100B and NSE serum markers were analyzed for their explanatory power for the DTI data, separately for FA, radial and axial diffusivity. For NSE, we did not obtain any significant results with the chosen statistical threshold. In contrast, serum levels of S100B were correlated with regional DTI parameters in female subjects, which was not the case for male.

TBSS results are presented in Figure 1. We show a significant negative correlation between S100B and FA across the anterior portion (rostrum, genu) and body of the corpus callosum, particularly the right anterior forceps, and the right superior longitudinal fasciculus (left upper row of Figure 1). No significant effects were detected for the posterior portions of the corpus callosum (splenium, tapetum). Additionally, we were able to show a significant positive correlation of S100B with radial diffusivity but not with axial diffusivity for the genu and anterior body of the corpus callosum, and for the anterior forceps (left lower row of Figure 1). In male subjects no such an association was detected – applying both corrected and uncorrected thresholds.

We aimed to confirm this result and compare female and male groups in a regional analysis focusing on the most consistent brain region, the corpus callosum. As illustrated in Table 1, VOI analyses revealed significant correlations in the female corpus callosum and therefore confirmed the previously described TBSS results. Interestingly, FA values were negatively correlated with S100B, whereas regional radial diffusivity was positively correlated with serum S100B. In men, we did not find any significant correlation with S100B and FA, radial or axial diffusivity measures using this regional approach. Furthermore, a permutation test with 100,000 permutations regarding S100B serum levels and FA/radial diffusivity revealed significant gender differences in women compared to men (Table 1).

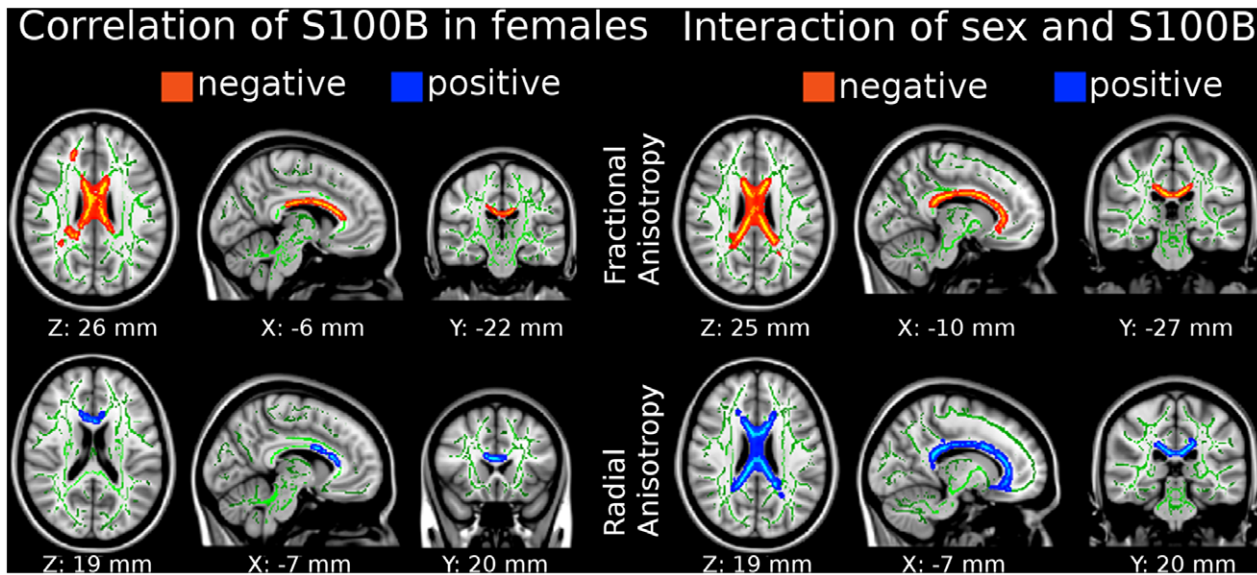


Figure 1. Diffusion tensor imaging parameters correlate with serum S100B mainly in the corpus callosum, anterior forceps, and the right superior longitudinal fasciculus of the female brain (left) in comparison with male brains (right). Clusters are corrected for multiple comparisons ($p < 0.05$, threshold-free cluster enhancement), positions are reported in MNI-coordinates. There was no significant correlation of S100B in male brains alone using multiple comparison correction and very little using uncorrected thresholds (not shown). Radiological convention (left side of the brain is presented on the right). doi:10.1371/journal.pone.0043284.g001

The same result, which was obtained by computing the interaction effect of females and males regarding S100B levels, can be seen on the right side of Figure 1. Here, we show a significant lower FA (upper row, right) in the anterior parts (rostrum, genu) and body of the corpus callosum, parts of the superior longitudinal fasciculus and anterior and posterior forceps, and a significantly higher radial diffusivity (lower row, right) in the genu, rostrum and body of the corpus callosum and the anterior forceps in females compared with males. In addition to the FA results, we show significant results analyzing radial diffusivity in regions of the left external capsula and left uncinata fasciculus.

Combining Serum Markers and T1-weighted Magnetic Resonance Imaging

Both S100B and NSE as glial/neuronal serum markers were analyzed for their explanatory power for T1-weighted MRI data, namely GM intensity. For S100B, we did not obtain any significant results with the chosen statistical threshold. In contrast, serum levels of NSE were correlated with regional GM density particularly in female subjects. Results of the VBM analysis are illustrated in Figure 2. We report data using a voxel-wise threshold of $p < 0.001$ and show clusters which remained significant after correction using a cluster-wise threshold of $p < 0.05$ family wise error (FWE). In female subjects, serum NSE was negatively correlated with GM density in the amygdalae and most anterior hippocampi bilaterally. No significant effects were obtained for male subjects with the chosen statistical threshold.

In a second step, we aimed to confirm this result and compare female and male groups in a regional analysis focusing onto the amygdalae. We computed a VOI analysis using the TD-ICBM Human Atlas in SPM and bilaterally selected the amygdaloid structures. These structures were used as masks for both, female and male groups, and smoothed GM values were extracted. Correlation of NSE and smoothed mean GM values, again corrected for covariates, were computed for both groups separately and can be seen in Table 2. Interestingly, both groups showed a significant negative correlation of GM density with NSE in the amygdaloid region in this VOI analysis – in contrast to the first whole-brain VBM analysis, where only females showed this association. Nonetheless, we failed to find significant gender differences using a permutation test with 100,000 permutations. We did not find any other significant correlation, difference or interaction of NSE and GM in any other group or combination of groups.

Table 1. Correlation values and permutation results for S100B, fractional anisotropy, radial and axial diffusivity in the corpus callosum.

sex	p-value	correlation coefficient	significance of difference between correlation coefficients
Fractional Anisotropy			
female	0.01	-0.59	p-value
male	0.26	0.3	0.004
Axial diffusivity (λ_{\parallel})			
female	0.91	-0.03	p-value
male	0.7	0.11	0.68
Radial diffusivity (λ_{\perp})			
female	0.01	0.61	p-value
male	0.22	-0.31	0.002

Note: Significant effects are written in bold. doi:10.1371/journal.pone.0043284.t001

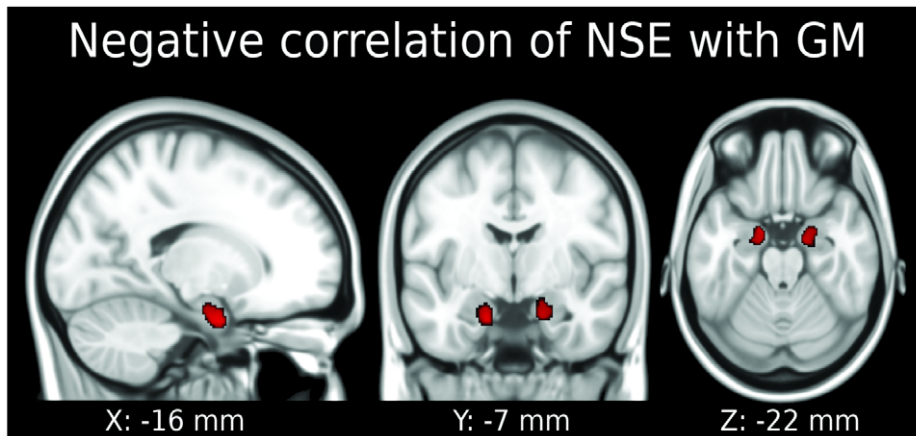


Figure 2. Gray matter density (GM) in both amygdalae and both most anterior hippocampi is correlated with serum neuron-specific enolase (NSE) in the female brain. No significant results were obtained for male subjects. $p < 0.05$ family wise error was applied, reported coordinates are MNI coordinates. Neurological convention (left side of the brain is presented on the left). doi:10.1371/journal.pone.0043284.g002

Histological and Whole Brain Gene Expression Analyses

In the histological study we examined co-localization between S100B and oligodendrocyte specific antigens in the human corpus callosum and cell culture by double immunofluorescence labeling. Figure 3 shows a close co-localization between S100B and oligodendrocyte specific myelin basic protein-positive myelinated fibres in the human corpus callosum, and between S100B and the oligodendrocyte/Schwann cell marker p75NTR in most oligodendroglial OLN-93 cells. Note that not all S100B positive cells are labelled as oligodendrocytes in Figure 3B as oligodendroglial markers are not expressed during all stages of oligodendrocyte development/maturation.

If we analyzed S100B gene expression in the whole human brain, S100B was most abundantly expressed in the corpus callosum, followed by the globus pallidus (Figure 3). The bar chart illustrates normalized z scores for these brain regions. All respective regions showed elevated S100B expression (Probe 1/2 corpus callosum $p = 0.006$, external globus pallidus $p < 0.05$, internal globus pallidus $p = 0.08/0.06$; 2-tailed Student's t test against 0), whereas there were no differences between probe 1 and 2 for each region warranting a high reliability ($p > 0.74$; unpaired 2-tailed Student's t test). Gene expression of S100B was, for both probes 1 and 2, higher in the corpus callosum than the external ($p = 0.048/0.036$) and internal globus pallidus ($p = 0.08/0.057$) without significant differences between both segments of the globus pallidus ($p > 0.6$).

Table 2. Correlation values and permutation results for serum neuron-specific enolase and averaged smoothed gray matter density in the amygdalae.

sex	<i>p</i> -value	correlation coefficient	significance of difference between correlation coefficients
female	0.0040	-0.66	<i>p</i> -value
male	0.0097	-0.62	0.5

Note: Significant effects are written in bold.
doi:10.1371/journal.pone.0043284.t002

Discussion

Our study aimed to validate the impact of serum markers on imaging data covering the GM and WM of the human brain. We focused on S100B because it is a glial protein that might act as a neuro- and gliotrophin inducing plasticity effects in the human brain [62–64].

As already stated in the introduction section we investigated the relationship between cell type specific serum markers and imaging parameters in a healthy cohort to exclude any impact of disease, because increased serum S100B may indicate glial alterations due to brain damage [65] in addition to functional secretion of S100B by astrocytes and/or oligodendrocytes [14]. Mathematical models suggest that serum S100B levels exceeding approximately 350 ng/l indicate brain damage [66]. Mathematical equations have been developed using values derived from literature and linearly fitting those values into a function in this study. Regarding neurological diseases with obvious brain damage, e.g. Creutzfeldt-disease, mean expression levels are significantly increased to 395 ng/l [67], or in traumatic brain injuries with bad prognosis above 500 ng/l [68]. Accordingly, literature data supports the mathematically derived threshold. Lower levels below 300 ng/l have been detected in neuropsychiatric disorders, such as depression or schizophrenia and might describe a regenerative action through S100B, and due to their low concentration less likely a neurodegenerative process [8,9]. Mean serum S100B was in the normal range of healthy subjects and far below this threshold in our subjects [45]. Likewise, normal NSE values exclude neuronal damage in our cohort [8,54].

Our study shows that S100B is specifically related to WM structures in the healthy human brain as it correlated negatively with FA. We observed this effect in female subjects only, which might be related to higher serum levels of S100B, higher variance and a wider range of values of this glial protein in the female study group compared to male subjects. Furthermore, to the authors' knowledge, there is no evidence to expect different expression pattern across sexes although our study shows significant correlations only within the female group. The results of the Allen Brain Atlas underpin the hypothesis of equal expression patterns across sexes, because all investigated subjects in this brain atlas are males, which show high S100B gene expression in the corpus callosum. Therefore, we conclude that due to the lower

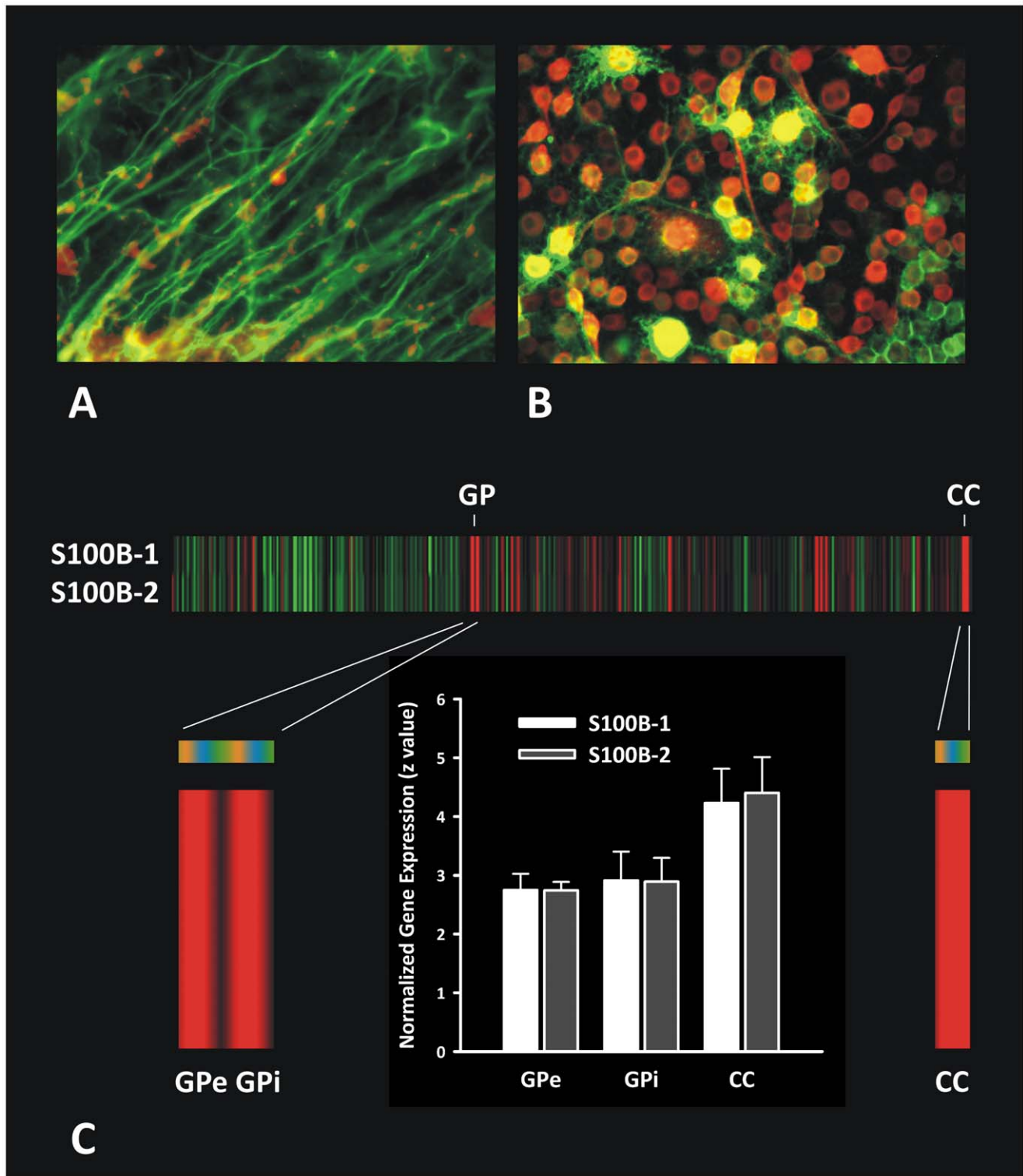


Figure 3. Expression and localization of S100B in the brain. (A) Co-localization (yellow) of S100B (red) and myelin basic protein (MBP)-positive (green) myelinated fibres in the human corpus callosum. Data originate from the subject previously published [6]. (B) Co-localization (yellow) between S100B (red) and the oligodendroglial marker p75 neurotrophin receptor (green) in the oligodendrocyte cell line OLN-93. (C) Individual normalized gene expression of S100B in heat map in z scores normalized to whole human brain expression, where green indicates relatively low and red relatively high expression. Subjects are coded in orange, blue and green (H351.2001,,2002 and.1009). Highest expression was detected in the corpus callosum (CC), followed by globus pallidus (GP). Bar chart shows quantitative values in CC and external/internal (e/i) GP (mean+standard deviation). Gene expression of S100B was analyzed in two probes: Probe 1 A_23_P143526; Sequence: AGCTTGATTTGCTTTGTGATTGAAAAATT-GAAAACCTTTTCCAAAGGCTGTTTTAACGG; Probe 2 CUST_17042_P1416261804; Sequence: AAGCTGAAGAAATCCGAAGTGAAGGAGCTCATCAACAAT-GAGCTTT CCCATTTCTTAGAG.
doi:10.1371/journal.pone.0043284.g003

range of S100B values in our male cohort, we failed to show a significant correlation.

Our second more specific analysis revealed that correlations of serum S100B with FA in women had to be attributed to a positive correlation with radial diffusivity in the same regions without significant effects for axial diffusivity. For the GM we did not obtain any significant correlations with S100B. Remarkably, in these analyses, we corrected for potential influences of neuronal influences on DTI or VBM parameters by including the neuronal marker protein NSE as a covariate. For NSE, we did generally not detect any significant correlations with DTI parameters.

The close positive correlation of serum S100B with radial diffusivity fits well with our post mortem histological double immunofluorescence data demonstrating a high concentration of S100B in oligodendrocytes in the healthy human brain, particularly in the corpus callosum, the dorsolateral prefrontal, parietal and temporal WM (see results and Steiner et al. (2007) [6]). Most interestingly, the Allen Brain Atlas, which provides gene expression data across the whole human brain, indicates highest expression of S100B in the corpus callosum in agreement with our results and in the globus pallidus in agreement with the literature [69].

In sum and to our knowledge, our study is the first one validating the specificity of the glial protein S100B for brain changes in vivo. Our results support the assumption that radial diffusivity represents a myelin marker, whereas axial diffusivity represents an axonal marker, as already shown in [43], although this topic is controversially discussed [70]. Although, all subjects were healthy we detected negative correlations with FA, which can be interpreted as a loss of directedness, and positive correlations with radial diffusivity which might be coupled with a loss in myelination. One should note that the obtained serum markers are whole brain measures and for the first time correlated with imaging data. Our study suggests that in healthy subjects S100B is expressed in region wise patterns, which corresponds with high S100B expression in corpus callosum and globus pallidus. High S100B is associated with a reduction of FA and increased λ_1 but does by no means support the idea of unhealthy or abnormal expression of S100B and/or diffusion parameters.

Beside DTI as WM parameter, both serum markers were analyzed in their explanatory power for T1-weighted MRI data by

correlating them with GM density. Serum NSE was negatively correlated with regional GM density mainly in the amygdalae of both sexes, most pronounced in female subjects. One has to keep in mind that we controlled for serum S100B as a covariate in this analysis. We did not obtain any significant results for S100B in this analysis, although it is well known that human astrocytes contain and express S100B [6]. This might be related to a lower signal-to-noise ratio in the GM as it is composed of several other cell types beside astrocytes. In contrast, the close association between S100B and WM DTI parameters was observed mainly in the corpus callosum, where numerous fibers are oriented in the same direction yielding a very high signal-to-noise ratio [44]. Additionally, histological investigations showed highest concentration of oligodendrocytes in white matter in the corpus callosum, which might be an explanation for our sensitivity and the observed TBSS results [6]. This leads to the conclusion that S100B as an oligodendrocytic marker is closely related with radial diffusivity. An alternative view postulating a close relationship between S100B and astrocytes in the corpus callosum is very improbable, because 93% of S100B positive cells in the corpus callosum represent oligodendrocytes [6]. The same holds true for other structures in the white matter.

One might conclude that our study indeed investigated the 'normal' relationship between cell type specific serum markers and imaging parameters. Our results open a new perspective for future studies investigating major neuropsychiatric disorders – in particular major depression and schizophrenia, which have been discussed to be characterized by glial pathology [8,47,71] and affecting brain regions identified in our study [72,73].

Acknowledgments

We thank Dr. Terri Gilbert from the Allen Institute for Brain Sciences for support in data analyses.

Author Contributions

Conceived and designed the experiments: KAJT AV MLS. Performed the experiments: KA JK JT MLS. Analyzed the data: DPS KM MLS. Contributed reagents/materials/analysis tools: DPS KA JK KM MLS. Wrote the paper: DPS KA JS KM MLS.

References

- Schroeter ML, Steiner J (2009) Elevated serum levels of the glial marker protein S100B are not specific for schizophrenia or mood disorders. *Mol Psychiatry* 14: 235–237.
- Schafer BW, Heizmann CW (1996) The S100 family of EF-hand calcium-binding proteins: functions and pathology. *Trends Biochem Sci* 21: 134–140.
- Poelmans G, Buitelaar JK, Pauls DL, Franke B (2011) A theoretical molecular network for dyslexia: integrating available genetic findings. *Mol Psychiatry* 16: 365–382.
- Donato R (1999) Functional roles of S100 proteins, calcium-binding proteins of the EF-hand type. *Biochim Biophys Acta* 1450: 191–231.
- Zimmer DB, Cornwall EH, Landar A, Song W (1995) The S100 protein family: history, function, and expression. *Brain Res Bull* 37: 417–429.
- Steiner J, Bernstein HG, Bielau H, Berndt A, Brisch R, et al. (2007) Evidence for a wide extra-astrocytic distribution of S100B in human brain. *BMC Neurosci* 8: 2.
- Rothermundt M, Peters M, Prehn JH, Arolt V (2003) S100B in brain damage and neurodegeneration. *Microsc Res Tech* 60: 614–632.
- Schroeter ML, Abdul-Khaliq H, Krebs M, Diefenbacher A, Blasig IE (2008) Serum markers support disease-specific glial pathology in major depression. *J Affect Disord* 111: 271–280.
- Schroeter ML, Abdul-Khaliq H, Krebs M, Diefenbacher A, Blasig IE (2009) Neuron-specific enolase is unaltered whereas S100B is elevated in serum of patients with schizophrenia - Original research and meta-analysis. *Psychiatry Research* 167: 66–72.
- Schroeter ML, Abdul-Khaliq H, Fruhauf S, Hohne R, Schick G, et al. (2003) Serum S100B is increased during early treatment with antipsychotics and in deficit schizophrenia. *Schizophr Res* 62: 231–236.
- Steiner J, Schroeter ML, Schiltz K, Bernstein HG, Muller UJ, et al. (2010) Haloperidol and clozapine decrease S100B release from glial cells. *Neuroscience* 167: 1025–1031.
- Schroeter ML, Abdul-Khaliq H, Diefenbacher A, Blasig IE (2002) S100B is increased in mood disorders and may be reduced by antidepressive treatment. *Neuroreport* 13: 1675–1678.
- Rothermundt M, Peters M, Wiesmann M, Hettich M, Abel S, et al. (2002) The neuroplasticity marker S100B in schizophrenia: Increased serum levels are associated with negative symptomatology. *Schizophr Res* 53: 152–153.
- Schroeter ML, Abdul-Khaliq H, Sacher J, Steiner J, Blasig IE, et al. (2010) Mood disorders are glial disorders: evidence from in vivo studies. *Cardiovasc Psychiatry Neurol* 2010: 780645.
- Lambert JC, Ferreira S, Gussekloo J, Christiansen L, Brysbaert G, et al. (2007) Evidence for the association of the S100beta gene with low cognitive performance and dementia in the elderly. *Mol Psychiatry* 12: 870–880.
- Steiner J, Bogerts B, Schroeter ML, Bernstein HG (2011) S100B protein in neurodegenerative disorders. *Clin Chem Lab Med* 49: 409–424.
- Stroick M, Fatar M, Ragoschke-Schumm A, Fassbender K, Bertsch T, et al. (2006) Protein S-100B - A prognostic marker for cerebral damage. *Curr Med Chem* 13: 3053–3060.
- Schmechel D, Marangos PJ, Brightman M (1978) Neurone-specific enolase is a molecular marker for peripheral and central neuroendocrine cells. *Nature* 276: 834–836.
- Kaiser E, Kuzmits R, Pregant P, Burghuber O, Worofka W (1989) Clinical biochemistry of neuron specific enolase. *Clin Chim Acta* 183: 13–31.
- Marangos PJ, Schmechel DE (1987) Neuron specific enolase, a clinically useful marker for neurons and neuroendocrine cells. *Annu Rev Neurosci* 10: 269–295.

21. de Kruijk JR, Leffers P, Menheere PPGA, Meerhoff S, Twijnstra A (2001) S-100B and neuron-specific enolase in serum of mild traumatic brain injury patients - A comparison with healthy controls. *Acta Neurologica Scandinavica* 103: 175–179.
22. Ingebrigtsen T, Romner B (2003) Biochemical serum markers for brain damage: a short review with emphasis on clinical utility in mild head injury. *Restor Neurol Neurosci* 21: 171–176.
23. Busnello JV, Leke R, Oses JP, Feier G, Bruch R, et al. (2006) Acute and chronic electroconvulsive shock in rats: effects on peripheral markers of neuronal injury and glial activity. *Life Sci* 78: 3013–3017.
24. Schaf DV, Tort AB, Fricke D, Schestatsky P, Portela LV, et al. (2005) S100B and NSE serum levels in patients with Parkinson's disease. *Parkinsonism Relat Disord* 11: 39–43.
25. Ashburner J, Friston KJ (2000) Voxel-based morphometry—the methods. *Neuroimage* 11: 805–821.
26. Smith CD, Chebrou H, Wekstein DR, Schmitt FA, Markesbery WR (2007) Age and gender effects on human brain anatomy: A voxel-based morphometric study in healthy elderly. *Neurobiology of Aging* 28: 1075–1087.
27. Good CD, Johnsrude I, Ashburner J, Henson RN, Friston KJ, et al. (2001) Cerebral asymmetry and the effects of sex and handedness on brain structure: a voxel-based morphometric analysis of 465 normal adult human brains. *Neuroimage* 14: 685–700.
28. Chen XH, Sachdev PS, Wen W, Anstey KJ (2007) Sex differences in regional gray matter in healthy individuals aged 44–48 years: A voxel-based morphometric study. *Neuroimage* 36: 691–699.
29. Karas GB, Burton EJ, Rombouts SARB, van Schijndel RA, O'Brien JT, et al. (2003) A comprehensive study of gray matter loss in patients with Alzheimer's disease using optimized voxel-based morphometry. *Neuroimage* 18: 895–907.
30. Brenneis C, Seppi K, Schocke MF, Muller J, Luginger E, et al. (2003) Voxel-based morphometry detects cortical atrophy in the Parkinson variant of multiple system atrophy. *Mov Disord* 18: 1132–1138.
31. Kassubek J, Juengling FD, Kioschies T, Henkel K, Karitzky J, et al. (2004) Topography of cerebral atrophy in early Huntington's disease: a voxel based morphometric MRI study. *J Neurol Neurosurg Psychiatry* 75: 213–220.
32. Pannacciulli N, Del Parigi A, Chen K, Le DS, Reiman EM, et al. (2006) Brain abnormalities in human obesity: a voxel-based morphometric study. *Neuroimage* 31: 1419–1425.
33. Colcombe SJ, Erickson KI, Scaif PE, Kim JS, Prakash R, et al. (2006) Aerobic exercise training increases brain volume in aging humans. *J Gerontol A Biol Sci Med Sci* 61: 1166–1170.
34. Maguire EA, Gadian DG, Johnsrude IS, Good CD, Ashburner J, et al. (2000) Navigation-related structural change in the hippocampi of taxi drivers. *Proc Natl Acad Sci U S A* 97: 4398–4403.
35. Draganski B, Gaser C, Busch V, Schuierer G, Bogdahn U, et al. (2004) Neuroplasticity: changes in grey matter induced by training. *Nature* 427: 311–312.
36. Pezawas L, Verchinski BA, Mattay VS, Callicott JH, Kolachana BS, et al. (2004) The brain-derived neurotrophic factor val66met polymorphism and variation in human cortical morphology. *J Neurosci* 24: 10099–10102.
37. Meyer-Lindenberg A, Nicodemus KK, Egan MF, Callicott JH, Mattay V, et al. (2008) False positives in imaging genetics. *Neuroimage* 40: 655–661.
38. Meyer-Lindenberg A, Straub RE, Lipska BK, Verchinski BA, Goldberg T, et al. (2007) Genetic evidence implicating DARPP-32 in human frontostriatal structure, function, and cognition. *J Clin Invest* 117: 672–682.
39. Basser PJ, Mattiello J, LeBihan D (1994) MR diffusion tensor spectroscopy and imaging. *Biophys J* 66: 259–267.
40. Smith SM, Jenkinson M, Johansen-Berg H, Rueckert D, Nichols TE, et al. (2006) Tract-based spatial statistics: voxelwise analysis of multi-subject diffusion data. *Neuroimage* 31: 1487–1505.
41. Basser PJ, Pierpaoli C (1996) Microstructural and physiological features of tissues elucidated by quantitative-diffusion-tensor MRI. *J Magn Reson B* 111: 209–219.
42. Kochunov P, Thompson PM, Lancaster JL, Bartzokis G, Smith S, et al. (2007) Relationship between white matter fractional anisotropy and other indices of cerebral health in normal aging: Tract-based spatial statistics study of aging. *Neuroimage* 35: 478–487.
43. Song SK, Sun SW, Ju WK, Lin SJ, Cross AH, et al. (2003) Diffusion tensor imaging detects and differentiates axon and myelin degeneration in mouse optic nerve after retinal ischemia. *Neuroimage* 20: 1714–1722.
44. Mueller K, Anwender A, Moller HE, Horstmann A, Lepsiens J, et al. (2011) Sex-dependent influences of obesity on cerebral white matter investigated by diffusion-tensor imaging. *PLoS One* 6: e18544.
45. Portela LVC, Tort ABL, Schaf DV, Ribeiro L, Nora DB, et al. (2002) The serum S100B concentration is age dependent. *Clin Chem* 48: 950–952.
46. Nygaard O, Langbakk B, Romner B (1997) Age- and sex-related changes of S-100 protein concentrations in cerebrospinal fluid and serum in patients with no previous history of neurological disorder. *Clin Chem* 43: 541–543.
47. Schroeter ML, Steiner J, Mueller K (2011) Glial pathology is modified by age in mood disorders—a systematic meta-analysis of serum S100B in vivo studies. *J Affect Disord* 134: 32–38.
48. Gazzolo D, Michetti F, Bruschetti M, Marchese N, Lituania M, et al. (2003) Pediatric concentrations of S100B protein in blood: age- and sex-related changes. *Clin Chem* 49: 967–970.
49. Holtkamp K, Buhren K, Ponath G, von Eiff C, Herpertz-Dahlmann B, et al. (2008) Serum levels of S100B are decreased in chronic starvation and normalize with weight gain. *J Neural Transm* 115: 937–940.
50. Steiner J, Walter M, Guest P, Myint AM, Schiltz K, et al. (2010) Elevated S100B levels in schizophrenia are associated with insulin resistance. *Mol Psychiatry* 15: 3–4.
51. Steiner J, Schiltz K, Walter M, Wunderlich MT, Keilhoff G, et al. (2010) S100B serum levels are closely correlated with body mass index: an important caveat in neuropsychiatric research. *Psychoneuroendocrinology* 35: 321–324.
52. van Engelen BG, Lamers KJ, Gabreels FJ, Wevers RA, van Geel WJ, et al. (1992) Age-related changes of neuron-specific enolase, S-100 protein, and myelin basic protein concentrations in cerebrospinal fluid. *Clin Chem* 38: 813–816.
53. Nygaard O, Langbakk B, Romner B (1998) Neuron-specific enolase concentrations in serum and cerebrospinal fluid in patients with no previous history of neurological disorder. *Scand J Clin Lab Invest* 58: 183–186.
54. Casmiro M, Maitan S, De Pasquale F, Cova V, Scarpa E, et al. (2005) Cerebrospinal fluid and serum neuron-specific enolase concentrations in a normal population. *Eur J Neurol* 12: 369–374.
55. Griswold MA, Jakob PM, Heidemann RM, Nittka M, Jellus V, et al. (2002) Generalized autocalibrating partially parallel acquisitions (GRAPPA). *Magn Reson Med* 47: 1202–1210.
56. Good CD, Johnsrude IS, Ashburner J, Henson RN, Friston KJ, et al. (2001) A voxel-based morphometric study of ageing in 465 normal adult human brains. *Neuroimage* 14: 21–36.
57. Maldjian JA, Laurienti PJ, Kraft RA, Burdette JH (2003) An automated method for neuroanatomic and cytoarchitectonic atlas-based interrogation of fMRI data sets. *Neuroimage* 19: 1233–1239.
58. Brandner FA (1933) A Test of the Significance of the Difference of the Correlation Coefficients in Normal Bivariate Samples. *Biometrika* 25: 102–109.
59. Smith SM, Nichols TE (2009) Threshold-free cluster enhancement: addressing problems of smoothing, threshold dependence and localisation in cluster inference. *Neuroimage* 44: 83–98.
60. Wakana S, Caprihan A, Panzenboeck MM, Fallon JH, Perry M, et al. (2007) Reproducibility of quantitative tractography methods applied to cerebral white matter. *Neuroimage* 36: 630–644.
61. Jones AR, Overly CC, Sunkin SM (2009) The Allen Brain Atlas: 5 years and beyond. *Nat Rev Neurosci* 10: 821–828.
62. Kligman D, Marshak DR (1985) Purification and characterization of a neurite extension factor from bovine brain. *Proc Natl Acad Sci U S A* 82: 7136–7139.
63. Winninghammajor F, Staecker JL, Barger SW, Coats S, Vaneldik LJ (1989) Neurite extension and neuronal survival activities of recombinant S100-Beta proteins that differ in the content and position of cysteine residues. *Journal of Cell Biology* 109: 3063–3071.
64. Haglid KG, Yang Q, Hamberger A, Bergman S, Widerberg A, et al. (1997) S-100beta stimulates neurite outgrowth in the rat sciatic nerve grafted with acellular muscle transplants. *Brain Res* 753: 196–201.
65. Abdul-Khalik H, Schubert S, Stoltenberg-Didinger G, Troitzsch D, Botcher W, et al. (2000) Protein S-100beta in brain and serum after deep hypothermic circulatory arrest in rabbits: relationship to perivascular astrocytic swelling. *Clin Chem Lab Med* 38: 1169–1172.
66. Marchi N, Cavaglia M, Fazio V, Bhudia S, Hallene K, et al. (2004) Peripheral markers of blood-brain barrier damage. *Clin Chim Acta* 342: 1–12.
67. Otto M, Wiltfang J, Schutz E, Zerr I, Otto A, et al. (1998) Diagnosis of Creutzfeldt-Jakob disease by measurement of S100 protein in serum: prospective case-control study. *BMJ* 316: 577–582.
68. Rainey T, Lesko M, Sacho R, Lecky F, Childs C (2009) Predicting outcome after severe traumatic brain injury using the serum S100B biomarker: results using a single (24h) time-point. *Resuscitation* 80: 341–345.
69. Cammermeyer J (1960) The Distribution of Oligodendrocytes in Cerebral Gray and White Matter of Several Mammals. *American Journal of Anatomy* 107: 107–114.
70. Schmierer K, Wheeler-Kingshott CA, Tozer DJ, Boulby PA, Parkes HG, et al. (2008) Quantitative magnetic resonance of postmortem multiple sclerosis brain before and after fixation. *Magn Reson Med* 59: 268–277.
71. Bernstein HG, Steiner J, Bogerts B (2009) Glial cells in schizophrenia: pathophysiological significance and possible consequences for therapy. *Expert Rev Neurother* 9: 1059–1071.
72. Sacher J, Neumann J, Funfstuck T, Soliman A, Villringer A, et al. (2011) Mapping the depressed brain: A meta-analysis of structural and functional alterations in major depressive disorder. *J Affect Disord*.
73. Whitford TJ, Savadjiev P, Kubicki M, O'Donnell IJ, Terry DP, et al. (2011) Fiber geometry in the corpus callosum in schizophrenia: evidence for transcallosal misconnection. *Schizophr Res* 132: 69–74.